Mineral mapping of the Aristarchus Plateau. Paul G. Lucey, Joshua T.S. Cahill, Karen R. Stockstill-Cahill, and B. Ray Hawke, Hawaii Institute of Geophysics and Planetology, University of Hawaii, Honolulu, HI 96822 (lucey@higp.hawaii.edu)

Introduction

The Aristarchus Plateau is one of the most geologically diverse regions on the Moon. The plateau is located (23.7°N 313°E) between Mare Imbrium and Oceanus Procellarum and consists of a tilting slab that is sloping downward to the north-northwest [1]. The Plateau exhibits the largest sinuous rille on the Moon, Vallis Schroteri, and is blanketed by a thick pyroclastic deposit [2]. The southeast edge of the plateau features the 40 km diameter Copernican crater Aristarchus that exposes fresh material from beneath the pyroclastic veneer. Apollo orbital geochemistry revealed a prominent Th anomaly at the Plateau, and more recent analysis of Lunar Prospector data show two Th anomalies, one centered on the crater and the other to the northwest near the Agricola Mountains just off the plateau [3]. Earth-based spectral reflectance measurements showed the presence of diverse and unusual highland assemblages, including lithologies dominated by high-Ca pyroxene, and localized deposits highly enriched in olivine [4]. Analysis of Clementine data confirmed these observations and mapped the extent of pyroxene-dominated and olivine-dominated rocks [1, 5]. *Lucey et al.* [4] attributed the Th anomaly to one of the pyroxene-rich spectral units exposed in the crater and suggested it was similar to the evolved quartz monzodiorite 15415. *Zhang and Jolliff* [6] argue that the nonmare rocks exposed by the crater represent compositional endmembers for the lunar crust related to late-stage intrusive activity within the Procellarum KREEP Terrane (PKT).

In this abstract we present quantitative mineralogic and chemical analysis of Clementine and Earth-based telescopic data to refine the understanding of compositions exposed on the plateau and within Aristarchus crater.

Method

Multispectral Mapping: We apply the method of *Lucey* [7] for deriving mineralogy from Clementine imaging, and extend this method to include the Clementine NIR data set. This method involves computing millions of spectral mixtures covering the plagioclase-orthopyroxene-clinopyroxene-olivine series at a compositional resolution of 5%, then using this large database as a lookup table to determine the mineralogic composition of each pixel. The mixture series are computed over a range of Mg-number (Mg/Mg+Fe) of 50 to 100 in 10 intervals, and optical space weathering parameters (nanophase iron and agglutinates) are varied in 46 steps corresponding to the range of very mature to very immature. The radiative transfer model used was published in its entirety in *Lawrence and Lucey* [8].

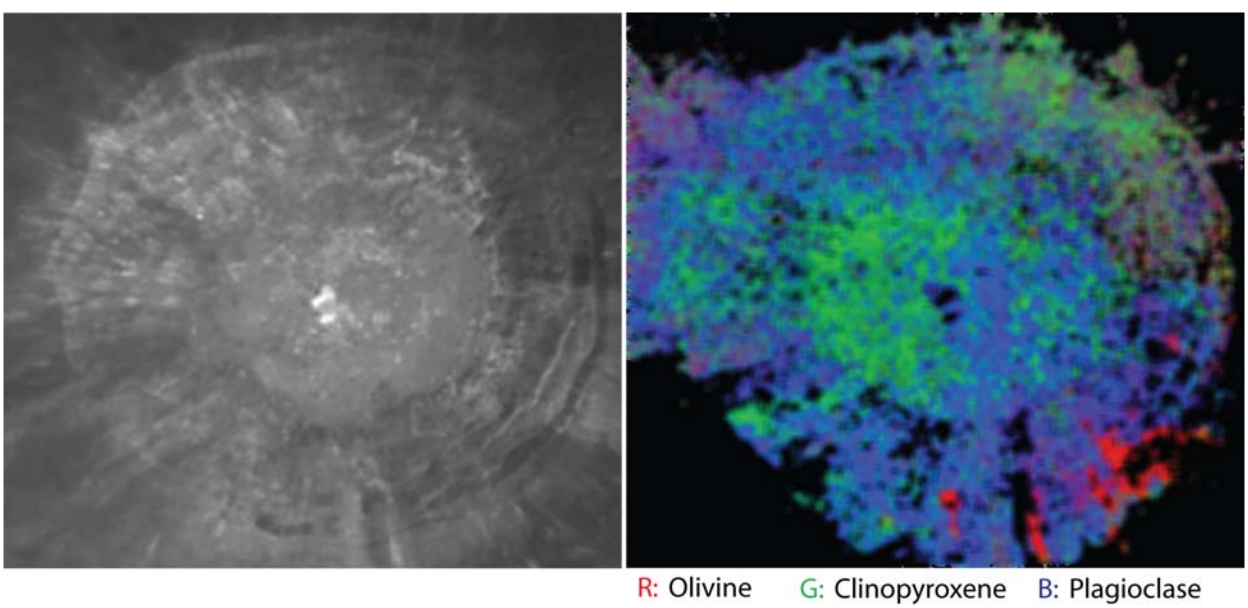

Figure 1: Displayed on the left is a Clementine 750 nm mosaic of Aristarchus crater (100 m/pixel). Shown on the right is an RGB image of modeled mineralogy deconvolved from immature (>0.3 in OMAT parameter) visible and near-infrared Clementine reflectance data.

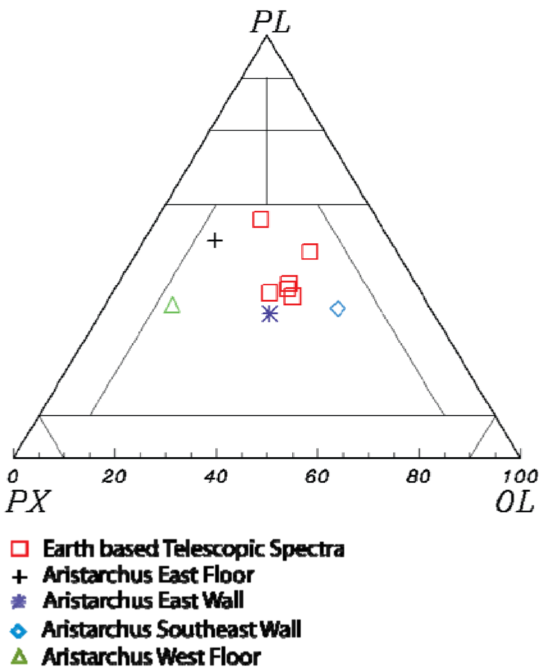

Figure 2: Plagioclase-pyroxene-olivine ternary diagram of Aristarchus Plateau modeled mineralogy for ground-based telescopic and orbital Clementine data.

Ground-Based Spectroscopy: Thirty-one spectra of the Aristarchus region collected by B.R. Hawke were used in this analysis some appearing in *Lucey et al.* [4]. The *Lawrence and Lucey* [8] model was used in concert with a gradient descent algorithm to model the normalized spectra of each location. Models were fit at 10 Mg-numbers, with mafic minerals sharing Mg-number, assuming an equilibrated composition. The final composition was that model that most closely matched the FeO content of the spectrum's location using the *Lawrence et al.* [9] calibration for deriving iron from multispectral imaging of the Moon.

Results

Multispectral Imaging: Mineral maps reveal several compositional units exposed within the crater, all being mafic, gabbroic and ferroan (Figure 1). The western floor and a portion of the western wall exposes a ferroan gabbro, with clinopyroxene to orthopyroxene ratio of 3 to 1 and a plagioclase content about 40 percent. Mg-numbers for this deposit can be relatively magnesian (70 to 85) but have a more ferroan average of 66. The southeastern wall and a small portion of the south wall reveal a more olivine-rich unit (Figure 1 and 2). Small portions of this deposit indicate magnesian troctolite areas, but most of the deposit is characterized with approximately equal portions of plagioclase and olivine and a more ferroan Mg' (~60).

The rest of the crater is more plagiclase-rich, but still within the gabbro field. The northeast wall of the crater appears to expose olivine-bearing mare basalt; the mineralogy at the location has approximately equal abundances of olivine and clinopyroxene, with minor orthopyroxene, a plagioclase content about 35 vol %, and FeO content about 18 wt%.

Ground-Based Spectroscopy: We analyzed several of the high quality spectra obtained of various locations within the crater [4] and one spectrum of the Agricola Mountains near the Th maximum revealed by [3]. Results are consistent with the multispectral imaging with all locations plotting within the gabbroic field (though Earth-based analyses indicate somewhat less cpx, with approximately equal abundances of cpx and opx). The methodology for the analysis of the continuous spectra are in active development, so these results may change.

Conclusions

The quantitative results presented here, based on comparisons with spectra computed using a radiative transfer mixing model, suggest the presence of rocks that are mineralogically gabbronorites, but with lower Mg'. The prominent Th anomaly strengthens this association (though at this time the Th cannot be unambigiuously attributed to any individual unit). Ferroan material detected includes both mare basalt, and possibly the original crust into which gabbros intruded.

References

[1] McEwen A.S., et al. (1994) *Science*, *266*, 1858-1862.
[2] Campbell B.A., et al. (2008) *Geology*, *36*, 135-138.
[3] Lawrence D.J., et al. (2007) *Lunar and Planetary Science Conference*, *38*, #1883.
[4] Lucey P.G., et al. (1986) *J Geophys Res-Solid*, *91*, D344-D354.
[5] Le Mouélic S., et al. (1999) *Geophys. Res. Lett.*, *26*, 1195-1198.
[6] Zhang J. and B.L. Jolliff (2008) *Lunar and Planetary Science Conference*, *39*, #2534.
[7] Lucey P.G. (2004) *Geophys. Res. Lett.*, *31*, doi:10.1029/2003GL019406.
[8] Lawrence S.J. and P.G. Lucey (2007) *J Geophys Res-Planet, doi:10.1029/2006JE002765.*
[9] Lawrence D.J., et al. (2002) *J Geophys Res-Planet*, *107*, 5130.